

LY293111 Improves Efficacy of Gemcitabine Therapy on Pancreatic Cancer in a Fluorescent Orthotopic Model in Athymic Mice¹

Rene Hennig^{*}, Jacinthe Ventura[†], Ralf Segersvard[†], Erin Ward[†], Xian-Zhong Ding[†], Sambasiva M. Rao[‡], Borko D. Jovanovic[§], Takeshi Iwamura[¶], Mark S. Talamonti[†], Richard H. Bell Jr.[†] and Thomas E. Adrian[†]

^{*}Department of Surgery, University of Heidelberg, Heidelberg, Germany; [†]Department of Surgery, Feinberg School of Medicine, Northwestern University, Chicago, IL, USA; Departments of [‡]Pathology, and [§]Preventive Medicine, Feinberg School of Medicine, Northwestern University, Chicago, IL, USA; [¶]Miyazaki Medical College, Miyazaki, Japan

Abstract

Pancreatic cancer has an abysmal prognosis because of late diagnosis and lack of effective therapeutics. New drugs are desperately needed. The present study determined the effect of the LTB₄ receptor antagonist, LY293111, on tumor growth and metastases in a fluorescent orthotopic model of pancreatic cancer. Pancreatic cancer cells (S2-013) with stable expression of enhanced green fluorescent protein were implanted into the duodenal pancreatic lobe of athymic mice. Animals were allocated to four groups (eight mice per group): control (no treatment); LY293111; gemcitabine; and LY293111 + gemcitabine. Monitoring of the surgical procedure and follow-up examinations at 2, 3, and 4 weeks after implantation to monitor tumor growth and metastases were performed using a fluorescence microscope and the reversible skin-flap technique. A staging and scoring system was developed to evaluate tumor progression, based on the TNM classification. Control animals developed end-stage disease with invasive cancer, metastases, and cachexia. Tumor growth and incidence of metastases were significantly reduced in all treated mice. However, combined treatment with LY293111 and gemcitabine was most effective. LY293111 is a novel therapeutic agent for pancreatic cancer, which improves the efficacy of gemcitabine. It is well tolerated and can be administered orally and, therefore, provides a new hope for patients suffering from pancreatic adenocarcinoma.

Neoplasia (2005) 7, 417–425

Keywords: Pancreatic cancer, LY293111, gemcitabine, GFP, orthotopic tumor model.

Introduction

Patients diagnosed with pancreatic cancer have to face a disease with an abysmal prognosis and little hope for cure because effective therapies are not available. Pancreatic cancer is the fourth leading cause of cancer death in both

men (after lung, prostate, and colon cancers) and women (after lung, breast, and colon cancers) in the United States, and the incidence of this disease has not declined. Indeed, it has increased in Japanese and African Americans over the last decades [1–3]. Mortality almost equals incidence and most patients die within 6 months after being diagnosed with this disease [1,4]. Potentially curative surgery can only be performed in about 20% of these patients because of metastatic spread or involvement of major blood vessels [4,5]. However, even in this selective group, the 5-year survival rate is only approximately 20% because of early tumor recurrence or metastatic tumor progression [6]. Gemcitabine is widely used as a standard therapy in pancreatic cancer patients in neoadjuvant, adjuvant, and palliative treatment protocols. However, besides improving quality of life, survival is only prolonged for about 1 month [7,8]. Therefore, new therapeutic strategies are urgently required for pancreatic cancer patients.

[2-Propyl-3-[3-[2-ethyl-4-(4-fluorophenyl)-5-hydroxyphenoxy]propoxy]phenoxy]-benzoic acid (LY293111) is a leukotriene B₄ (LTB₄) receptor antagonist, which showed marked growth inhibition of human pancreatic cancer cells *in vitro* and in subcutaneous xenograft models, inducing apoptosis and S-phase arrest [9]. Recently, it has been shown that LTB₄ receptors are overexpressed in human pancreatic cancer cells and tissues [10]. Moreover, LTB₄ stimulates the growth of human pancreatic cancer cells by inducing ERK1/2 phosphorylation, which can be inhibited by LY293111 [11,12]. LTB₄ is a final product of the arachidonic acid—metabolizing 5-lipoxygenase (5-LOX) pathway and is well-known as a biologic mediator in several chronic inflammatory diseases as asthma, psoriasis, rheumatoid arthritis, and inflammatory bowel disease [13,14]. As in other cancers, cyclooxygenase-2 (COX-2) plays a role in the growth and spread

Address all correspondence to: Thomas E. Adrian, PhD, FRCPath, Department of Surgery, Northwestern University, Tarry Building, 4-711, 303 East Chicago Avenue, Chicago, IL 60611. E-mail: tadrian@northwestern.edu

¹This work was supported by grants from the National Cancer Institute SPORE program (CA72712), the American Institute for Cancer Research (00B065), and the Lilly Research Laboratories. R.H. received a fellowship award from the Deutsche Forschungsgemeinschaft. Received 18 August 2004; Revised 3 January 2005; Accepted 4 January 2005.

Copyright © 2005 Neoplasia Press, Inc. All rights reserved 1522-8002/05/\$25.00
DOI 10.1593/neo.04559

of pancreatic cancers [15]. However, the 5-LOX pathway seems to play an even more important role in pancreatic cancer growth and development [15,16]. The LTB₄ antagonist activity of LY293111 was evaluated previously in clinical testing for inflammatory conditions [17–20]. Although it was found to be safe and well-tolerated, the development of the drug for inflammatory conditions was discontinued [21].

However, to bring new treatments from the laboratory into the clinic, adequate *in vivo* studies are required. The subcutaneous xenograft model for pancreatic cancer is limited because the tumor is growing in an unusual environment (subcutaneous) without high concentrations of important growth factors, such as insulin. There are also differences in tumor biology and morphology in this xenotopic site [22,23]. Therefore, in the current study, we used an orthotopic tumor model in athymic mice to determine the effectiveness of LY293111 alone and in combination with gemcitabine *in vivo*. This model employs S2-013 cells with stable transfection of green fluorescent protein (GFP). Because the tumors grow in their natural tissue environment, they develop metastases and mimic the clinical course of pancreatic cancer with obstruction of the duodenum and bile duct, and induction of cachexia. Moreover, the S2-013 human pancreatic cancer cell line was chosen among several others because of its metastatic potential and high aggressiveness to challenge the effectiveness of LY293111. The fluorescent model enables dynamic monitoring of tumor growth and metastases under different therapeutic strategies [24,25].

Materials and Methods

Cell Lines and Cell Cultures

S2-013, a subclone of SUIT-2, is a well-differentiated cell line derived from a liver metastasis of human pancreatic adenocarcinoma [26–28]. These cells were stably transfected with enhanced GFP and provided by Dr. M.A. Hollingsworth (Eppley Cancer Institute, Omaha, NE). The cells were cultured in Dulbecco's modified Eagle's medium (DMEM), supplemented with 10% fetal bovine serum, 100 U/ml penicillin, 100 µg/ml streptomycin, and 0.25 µg/ml amphotericin B (Cellgro; Mediatech, Inc., Herndon, VA). S2-013 tumor cells were harvested from 90% confluent cultures grown in T75 flasks (Corning, Inc., Corning, NY). The tumor cells were trypsinized, then the cell number was counted using a Guava Personal Cytometer (Guava Technologies, Inc., Hayward, CA) and resuspended in DMEM.

Animals and Surgical Orthotopic Tumor Cell Implantation (SOI)

Thirty-two 6- to 8-week-old female athymic nude (nu/nu) mice purchased from the National Cancer Institute were used in this study. The mice were housed in a two-way barrier facility in microisolator cages on static racks, fed with autoclaved laboratory rodent food pellets and acclimatized to the facility for 1 week before SOI. Animal weight was recorded everyday. Their use in this study was approved by the Institutional Animals Care and Use Committee and all

procedures were conducted in accordance with the regulations and standards of the National Institutes of Health.

Mice were anesthetized intraperitoneally with 0.05 ml of a mixture of 0.4 ml of ketamine (Fort Dodge Animal Health, Fort Dodge, IO), 0.1 ml of xylazine (Phoenix Scientific, Inc., St. Joseph, MO), and 0.5 ml of NaCl. The abdomen was sterilized with alcohol pads and a 0.5-cm midline incision was performed. The abdominal wall was wrapped with wet gauze. After pulling the stomach on the surface, the pancreas was then carefully exposed and tumor cells (5×10^5 in 10 µl of DMEM) were injected into the duodenal lobe using a monoject 200 27-gauge \times 1/2 in. polypropylene hub hypodermic needle (Kendall, Mansfield, MA) and a 50-µl glass syringe (Hamilton Company, Reno, NV). The needle was carefully withdrawn and the injection sealed with a dry cotton tip. The successful injection was confirmed using a stereo fluorescence microscope. After the stomach and pancreas were returned to the peritoneal cavity, the incision was closed in two layers with vicryl-coated Rapide sutures 4-0 (Ethicon, Inc., Somerville, NJ). Once the mice were ambulatory, they were placed in the animal barrier facility. The mice were kept in a sterile environment throughout the procedure.

Therapy

One day after SOI, the mice were randomized into four groups: Group I (Control) received daily oral doses of the vehicle, DMSO (1/2 µl/g per day); Group II (LY293111) received daily oral doses of LY293111 (250 mg/kg per day, dissolved in DMSO and administered 1/2 µl/g per day); Group III (Gemcitabine) received daily oral dosages of DMSO (1/2 µl/g per day) and intraperitoneal injections of gemcitabine (60 mg/kg per dose dissolved in PBS and administered 2 µl/g per day) on days 4, 7, 10, and 13 after SOI; and Group IV (LY293111 + gemcitabine) received daily oral dosages of LY293111 (250 mg/kg per day) and intraperitoneal injections of gemcitabine (60 mg/kg per dose) on days 4, 7, 10, and 13 after SOI. LY293111 and gemcitabine were provided by Eli Lilly (Indianapolis, IN). Eight mice were assigned to each group and treated for 4 weeks, at which time the experiment was terminated and animals were euthanized.

Surgical Follow-Up Procedures

The mice underwent follow-up procedures 2 weeks after SOI. Mice were anesthetized with the same mixture of ketamine, xylazine, and NaCl. A horizontal arc-shaped incision was made through the skin and connective tissue was bluntly separated from the peritoneum with a curved scissors to free the skin flap (reversible skin flap) [29]. Digital pictures of tumors were taken with and without fluorescence, and staging of peritoneal tumors, pancreatic tumors, lymph node metastases, liver metastases, and ascites was performed and recorded according to our TMPN scoring system (Table 1, Figure 1). The scores from each category were multiplied with each other because patterns in medicine follow multiplicative, rather than additive, rules. The incision was closed with vicryl-coated Rapide 4-0 sutures. Follow-up surgeries were performed in the second, third, and fourth weeks after SOI.

Table 1. TMPN Classification and Scoring System.

Staging and Scoring System		
Stage	Description	Score
<i>Primary tumor</i>		
T ₀	No tumor	1
T ₁	Small tumor (tumor $d < 7$ mm)	2
T ₂	Large tumor without infiltration (tumor $d > 7$ mm)	3
T ₃	Large tumor with infiltration but still visible margins	4
T ₄	Diffuse and infiltrating tumor	5
<i>Organ metastases</i>		
M ₀	No liver or lung metastases	1
M _{1Li}	Liver metastases	5
M _{1Lu}	Lung metastases	5
M ₁	Liver and lung metastases	10
<i>Peritoneal metastases</i>		
P ₀	No peritoneal metastases	1
P ₁	Less than five peritoneal metastases or one with $d < 7$ mm	3
P ₂	More than five peritoneal metastases or one with $d > 7$ mm	4
P ₃	Malignant ascites	5
<i>Lymph node metastases</i>		
N ₀	No lymph node metastases	1
N ₁	Peripancreatic lymph node metastases	3
N ₂	Regional lymph node metastases (e.g., mesenteric, Virchow)	5

Scores for the primary tumor (T), organ metastases (M), peritoneal metastases (P), and lymph node metastases (N) were multiplied to calculate the total tumor score for each animal.

After the last follow-up, mice were euthanized using a higher dose of the same mixture of ketamine, xylazine, and NaCl (0.1 ml). A midline skin incision was made from the area just above the bladder to the clavicles and the connective tissue was separated. After staging and imaging using the stereo fluorescence microscope, ascites was collected. If no ascites was accessible by abdominal puncture, a brushing of the peritoneal cavity was taken with a cotton-tipped applicator (Henry Schein, Inc., Melville, NY) and smeared onto a microscope slide. Staging and imaging were performed before and after opening the peritoneum and thoracic cavity. From each mouse, peritoneal tumor, pancreatic tumor, lymph node, liver, and lung tissues were harvested and fixed in 4% formaldehyde for 12 hours. Prior to fixation, peritoneal and pancreatic tumors were weighed and measured in length and width and the tumor volume calculated as follows: volume = (length) \times (width) \times (length + width/2) \times 0.526. The whole pancreas was collected en bloc with tumor, 5 mm of the proximal duodenum and the whole stomach. The stomach was cut and emptied, and the entire cluster of tissues was weighed, whereas only the pancreatic tumor was measured. Liver, lung, and thoracic lymph node tissues were further checked for any metastases with the stereo fluorescence microscope at higher magnification and photographed. After 12 hours of tissue fixation, 4% formaldehyde was replaced with 70% ethanol, and tissues were then paraffin-embedded according to histology standard protocols.

Imaging

Images were taken with a Nikon stereoscopic zoom microscope model SMZ1500 equipped with a DC10NN

high-resolution video camera and a 100-W mercury lamp (Nikon Instruments, Inc., Melville, NY). A tungsten halogen lamp (Schott-Fostec, LLC, Auburn, NY) with a variable powered output of 150 W of light was also used. Selective excitation of GFP was produced through a HQ480/40 band-pass filter and 495 dichroic mirror. Emitted fluorescence was collected through a longpass 500 filter. Images were processed and analyzed using Image Pro Plus 4.5 software (Media Cybernetics, Silver Spring, MD).

Histology

Hematoxylin and eosin (H&E) staining with Gill's Hematoxylin (Fisher Scientific, Fair Lawn, NJ) and Eosin Y (American Master Tech Scientific, Inc., Lodi, CA), each for 5 minutes, was used for routine staining of 4- μ m tissue sections. Histologic evaluation was performed under light microscopy. Sections were mounted with Permount (Fisher Scientific).

Statistical Analysis

Tumor staging scores, tumor weight, and tumor volume were compared using ANOVA as a parametric test and Kruskal-Wallis ANOVA on ranks as a nonparametric test. Student-Newman-Keuls was used as post-hoc test. Fisher's exact test was used to compare differences in the frequency of metastases. Data from all 32 animals were statistically analyzed and differences were considered as statistically significant when $P < .05$. Graphs were created using the GraphPad Prism Software.

Results

Tumor Model S2-013 GFP

S2-013 is a highly aggressive, invasive, and spontaneously metastasizing human pancreatic cancer cell line. Using our injection technique, we were able to target injection of the tumor cells into a discrete region of the duodenal lobe of the pancreas without leakage. Success of each injection was confirmed by stereo fluorescence microscopy (Figure 1). Untreated animals develop an end-stage disease within 4 weeks after SOI and present with a primary tumor invading neighboring tissues; obstructing the duodenum and bile duct; metastasizing to the lymph nodes, liver, and lung; and causing peritoneal carcinomatosis with malignant ascites and cachexia (Figure 1). Therefore, injecting S2-013 GFP tumor cells into the duodenal lobe of the pancreas mimics the clinical features of human pancreatic adenocarcinoma. The technical approach was very reliable and tumor formation was seen in all animals. The GFP expression of the cells enabled us to dynamically monitor primary tumor growth and the development of metastases, and therefore to compare disease stages under different therapeutic strategies (Figure 1).

Body Weight

Body weights between the four groups were not significantly different throughout the experiment. It should be noted that the measured body weights at the end of the

experiment do not fully reflect the nutritional state of the animals because of different tumor loads and volumes of ascites. After correcting body weights for these values, we observed a 1.2-g increase in gemcitabine-treated animals between the beginning and end of the experiment. The untreated mice as well as animals under treatment with LY293111 alone lost between 1.4 or 2 g of body weight, whereas weights of mice receiving the combined therapy of gemcitabine and LY293111 remained stable.

Tumor Staging

According to the TNM classification, we developed a scoring system that was used to perform a weekly staging of the disease. Tumor staging systems have not been used in previous orthotopic tumor models, so effectiveness of novel anticancer therapeutics was rather descriptive and observer-dependent. The tumor scores showed significant differences between treated groups and the control group in all follow-ups, with the highest score in control animals and the lowest score in animals treated with the combination of LY293111 and gemcitabine (Figure 2). LY293111 alone was the least effective treatment (Figure 2). However, the tumor score was lower compared to controls, a difference that was significant in the fourth week after SOI (Figure 2). Animals treated with gemcitabine alone or in combination with LY293111 showed significantly lower tumor scores than the control and LY293111 groups at all follow-ups (Figure 2). Moreover, the combined treatment of gemcitabine and LY293111 proved to be significantly better than gemcitabine alone with regard to tumor scores at weeks 3 and 4 after SOI (Figure 2), suggesting a benefit from combining LY293111 with gemcitabine.

Duodenal obstruction was not included in the scoring system. The decision as to whether or not the duodenum is obstructed was made when a tumor was strangulating the pylorus or duodenum and the stomach was distended. Four of eight animals in the control group, three of eight in the LY293111 group, and one of eight in the gemcitabine group showed duodenal obstruction, whereas none of the animals treated with LY293111 and gemcitabine suffered from this clinical feature.

Tumor Weight and Volume

The measurements of tumor weight and calculations of tumor volume for the primary tumor in the pancreas and peritoneal metastases revealed similar results and the same pattern of therapeutic effectiveness as was obtained with the tumor scores. All three treated groups had a significantly lower tumor weight and volume of the primary tumor compared to control, whereas no significant differences between these different treatment options were observed (Figure 3). However, LY293111 alone was again the least effective therapy and LY293111 + gemcitabine appeared to be most effective (Figure 3). Because of highly invasive tumors, particularly in the untreated animals, it was not possible to completely separate the tumor from adjacent organs. The weight of a whole tissue cluster consisting of the pancreas, empty stomach, and 5 mm of proximal duodenum

was measured in all 32 animals. Thus, the primary "tumor weight" in all groups includes the weight of these adjacent tissues. Tumor weights and volumes of peritoneal metastases were also markedly decreased, particularly following treatment with gemcitabine alone or in combination with LY293111; however, this did not reach statistical significance (Figure 4).

Hepatic and Lung Metastases

Five of eight untreated animals developed liver and lung metastases, whereas one mouse showed only lung metastases and two others showed no metastases (Figure 5). Treatment with LY293111 or gemcitabine decreased the incidence of lung metastases to three in each group, whereas only one animal in the LY293111 + gemcitabine group developed lung micrometastases (Figure 5). It should be mentioned that the technical problem of peritoneal leakage of tumor cells during SOI was recorded in this animal; however, it was decided that it should not be excluded from the study. Even more interesting is that only two animals treated with LY293111 had liver metastases, whereas gemcitabine alone or in combination with LY293111 completely eliminated the occurrence of liver metastases (Figure 5). Overall, except in one animal where we recorded technical problems in SOI, only the combined therapy with LY293111 and gemcitabine seems to be able to completely prevent the development of liver and lung metastases (Figure 5). However, statistical significance was reached only at a 10% α level ($P = .0844$).

Histology

Histologic examination of primary tumor, liver, lung, and lymphatic tissues from all animals was carried out by light microscopy at the end of the experiment. The pancreatic tumors showed the morphology of a poorly differentiated pancreatic adenocarcinoma, invading peripancreatic lymph nodes and neighboring organs. The metastases in the liver, lung, and lymph nodes observed by stereo fluorescence microscopy were confirmed histologically. Liver metastases appeared to develop from migration of tumor cells by blood and lymphatic vessels into the liver because tumor cells were seen in the lumens of hepatic blood and lymphatic vessels (Figure 1).

Discussion

Gemcitabine is the standard palliative treatment in unresectable pancreatic cancers and is the usual therapeutic baseline in adjuvant and neoadjuvant clinical trials, attempting to improve on the desperate situation of pancreatic cancer patients. Pancreatologists all over the world are looking for a beneficial drug to combine with gemcitabine. Taking all of the data together, the combined therapy of gemcitabine and LY293111 potentially inhibits the growth and metastases of this very rapidly growing and aggressive pancreatic adenocarcinoma. Sun et al. [30] reported that gemcitabine at a dose of 300 mg/kg per dose injected three times could not inhibit the development of lung metastases compared to untreated

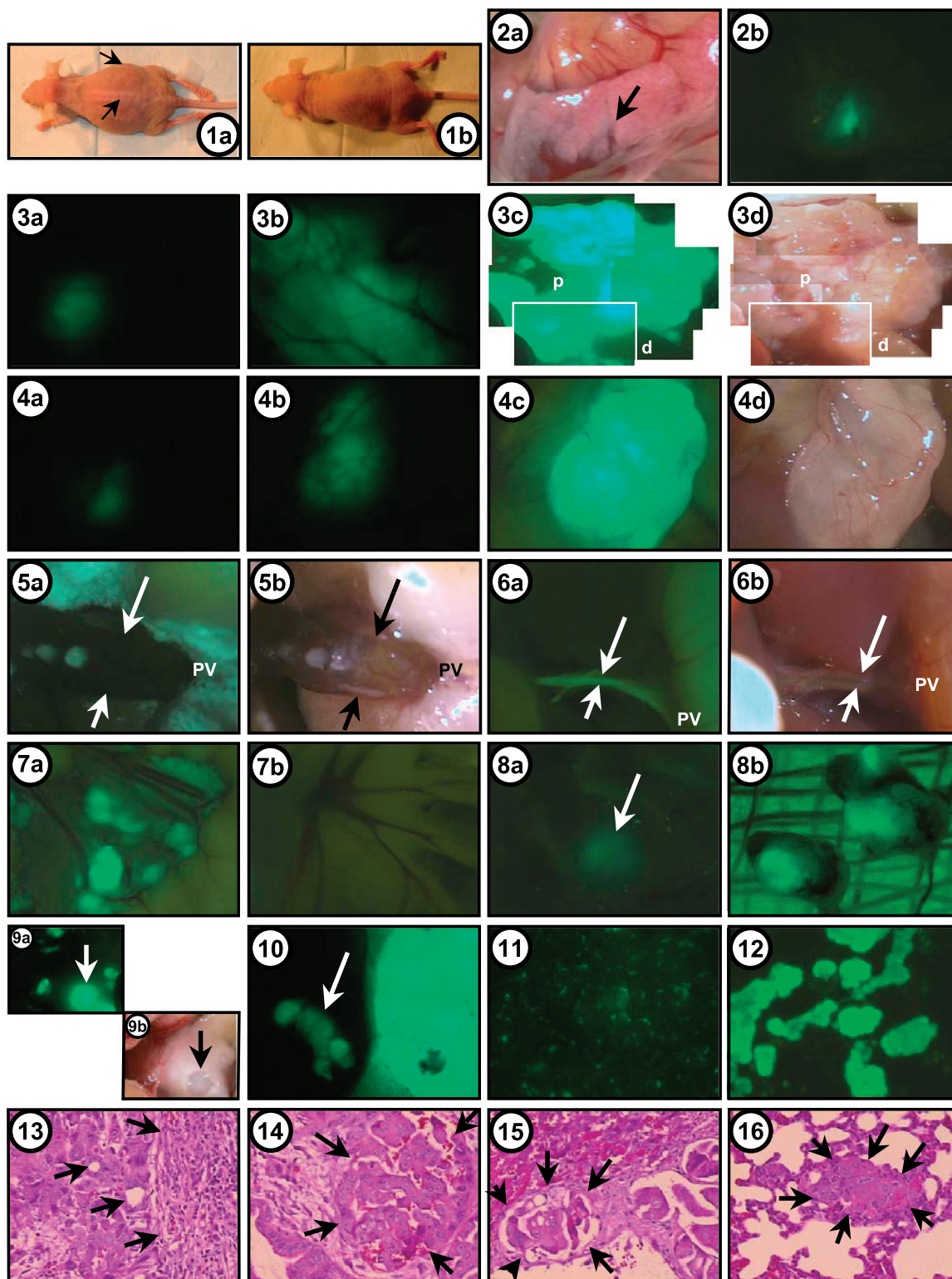


Figure 1. A summary of optical images is shown, captured by a digital video camera–equipped stereo fluorescence microscope and light microscope. Four weeks after SOI: (1a) untreated mouse with cachexia and ascites; (1b) normal looking-mouse treated with LY293111 and gemcitabine; (2) confirmation of SOI of S2-013 GFP cells into the duodenal lobe of the pancreas by (a) light and (b) fluorescent microscopy ($\times 7.5$); (3) growth of a primary tumor in (a) the second, (b) third, and (c + d) fourth weeks after SOI in an untreated control animal (3c + d: eight pictures with $\times 7.5$ magnification capture the tumor; p = pylorus, d = duodenum); (4) primary tumor growth in (a) the second, (b) third, and (c + d) fourth weeks after SOI from an animal treated with LY293111 and gemcitabine ($\times 7.5$); (5a + b) grossly distended bile duct in a control mouse and (6a + b) normal bile duct without tumor in an LY293111 and gemcitabine–treated mouse ($\times 7.5$; PV = papilla Vateri); (7a) mesenteric lymph node metastases in a control animal and (7b) normal mesentery in a LY293111 and gemcitabine–treated animal ($\times 7.5$); (8) intrathoracic lymph node metastasis in a control animal visualized (a) through the chest wall ($\times 7.5$) and (b) extirpated on gauze ($\times 20$); (9a + b) peripancreatic lymph node metastases ($\times 7.5$); (10) liver metastasis ($\times 7.5$) and (11) lung micrometastases in a control animal ($\times 20$); (12) malignant ascites in a control animal; (13) primary pancreatic tumor with desmoplastic reaction and duct-like tumor structures; liver metastases with (14) intravascular and (15) intralymphatic tumor cells; and (16) lung micrometastasis (12–16, all from a control animal, $\times 200$; 13–16, H&E–stained).

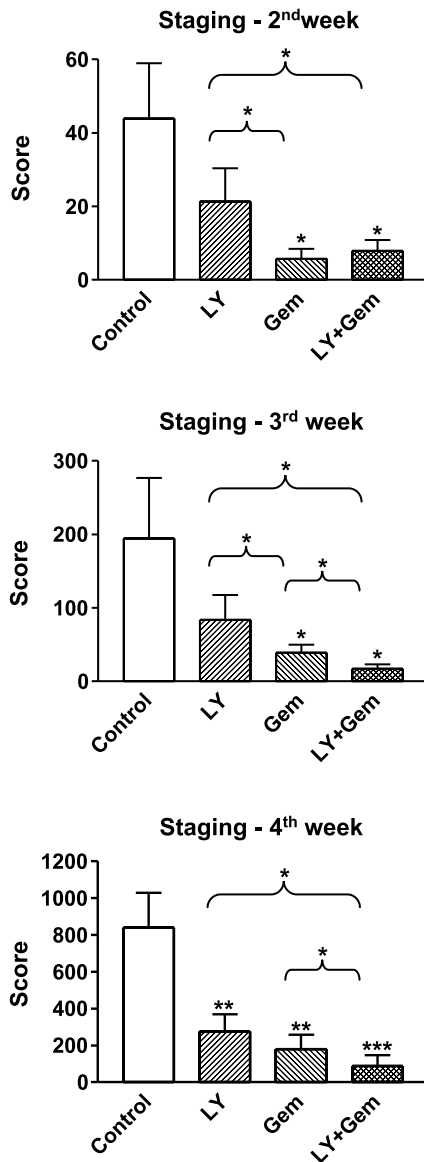


Figure 2. Tumor scores (mean ± SEM) in the second, third, and fourth weeks after SOI of S2-013 GFP human pancreatic cancer cells are shown. Groups include control; LY293111 (LY); (250 mg/kg per day); gemcitabine (Gem) (60 mg/kg per dose); and combined LY293111 and gemcitabine (LY + Gem) therapy. All P values are shown in Table 2.

controls. However, in our tumor model, gemcitabine at a dose of 60 mg/kg per dose injected four times to some extent inhibited the occurrence of lung metastases while completely eliminating liver metastases. The efficacy of gemcitabine in preventing metastases was markedly improved in combination with LY293111. Nevertheless, it should be mentioned that we started treatment with LY293111 from the first, and gemcitabine from the fourth, day after SOI because of this highly aggressive S2-013 tumor model, with rapid cancer development in all animals used. However, the treatment strategy of gemcitabine and LY293111 significantly delayed the progression of human pancreatic cancer in this orthotopic nude mouse tumor model. Moreover, LY293111 can be administered orally and showed no apparent toxicity; there-

fore, patient compliance could be expected. Body weight did not significantly differ between the experimental groups at any time during the experiment. It might be anticipated that the cachectic animals in the control group would have lost weight during the latter stages of the disease; however, the substantial tumor burden and volume of ascites substantially contributed to total body weight in this group. Furthermore, an increase in body weight might also have been expected in the groups treated with LY293111 compared with their respective controls, but this was not seen. Because of the problem with measuring body weight in fully ambulatory animals, the measurement is inherently noisy. If a small effect of LY293111 on food intake or body weight gain had occurred, it was not revealed in the present study. The condition of the animals with hepatic and lung metastases is very much worse than that of animals with only lymph node metastases. Indeed, the experiments were terminated because of the poor condition of the control animals, and this was part of the institutional animal care protocol.

Thus, combined therapy of gemcitabine + LY293111 could be a promising approach in treating pancreatic adenocarcinoma. This therapeutic strategy should be considered for neoadjuvant, adjuvant, and palliative clinical trials in pancreatic cancer patients because there is a significant

Table 2. Summary of Statistical Data.

Comparison	ANOVA	Kruskal	Fisher's	Normality Test
Pancreatic tumor volume	<i>P</i> = .004	<i>P</i> = .007		Failed
C versus LY	<i>P</i> = .056	<i>P</i> < .05		
C versus Gem	<i>P</i> = .006	<i>P</i> < .05		
C versus LY&Gem	<i>P</i> = .006	<i>P</i> < .05		
Peritoneal tumor volume	<i>P</i> = .023	<i>P</i> = .114		Failed
C versus Gem	<i>P</i> = .039			
C versus LY&Gem	<i>P</i> = .026			
Pancreatic tumor weight	<i>P</i> = .001	<i>P</i> = .004		Passed
C versus LY	<i>P</i> = .016	<i>P</i> < .05		
C versus Gem	<i>P</i> = .005	<i>P</i> < .05		
C versus LY&Gem	<i>P</i> = .001	<i>P</i> < .05		
Peritoneal tumor weight	<i>P</i> = .038	<i>P</i> = .058		Passed
Staging second week	<i>P</i> = .022	<i>P</i> = .019		Failed
C versus LY	<i>P</i> = .088			
C versus Gem	<i>P</i> = .029	<i>P</i> < .05		
C versus LY&Gem	<i>P</i> = .024	<i>P</i> < .05		
LY versus Gem		<i>P</i> < .05		
LY versus LY&Gem		<i>P</i> < .05		
Staging third week	<i>P</i> = .043	<i>P</i> = .01		Failed
C versus Gem		<i>P</i> < .05		
C versus LY&Gem	<i>P</i> = .044	<i>P</i> < .05		
LY versus Gem		<i>P</i> < .05		
LY versus LY&Gem		<i>P</i> < .05		
Gem versus LY&Gem		<i>P</i> < .05		
Staging fourth week	<i>P</i> < .001	<i>P</i> = .007		Passed
C versus LY	<i>P</i> = .002	<i>P</i> < .05		
C versus Gem	<i>P</i> = .001	<i>P</i> < .05		
C versus LY&Gem	<i>P</i> < .001	<i>P</i> < .05		
LY versus LY&Gem		<i>P</i> < .05		
Gem versus LY&Gem		<i>P</i> < .05		
Total metastases			<i>P</i> = .084	
Liver metastases			<i>P</i> = .006	
Lung metastases			<i>P</i> = .122	

P values for comparisons.

ANOVA as parametric and Kruskal-Wallis as nonparametric test.

C = control; LY = LY293111; Gem = gemcitabine; LY&Gem=LY293111 and gemcitabine.

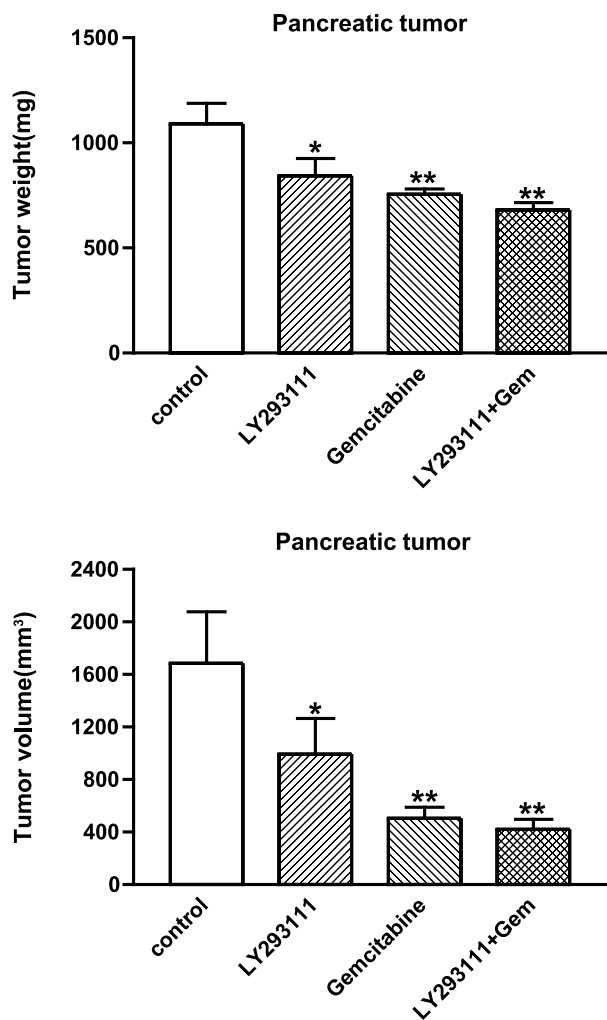


Figure 3. Primary pancreatic tumor weights and volumes (mean \pm SEM) 4 weeks after SOI of S2-013 GFP human pancreatic cancer cells. Groups include control; LY293111 (LY); (250 mg/kg per day); gemcitabine (Gem) (60 mg/kg per dose); and combined LY293111 and gemcitabine (LY + Gem) therapy. All P values are shown in Table 2.

beneficial effect of adding LY293111 to gemcitabine treatment. This benefit was seen even though gemcitabine alone is very effective in this model. LY293111 seems to have an additional, rather than a synergistic, effect to gemcitabine. In the present study, we do not claim tumor regression because this is particularly difficult in pancreatic cancer because of the marked desmoplastic reaction. Even gemcitabine does not induce tumor regression in most patients with this disease. According to the present study, LY293111 may be particularly valuable for patients undergoing potentially curative surgery, but may also be useful for patients desperately looking for better palliative treatment strategies than gemcitabine alone. The high compliance of cancer patients can be assumed to be due to oral availability and minor side effects.

The molecular mechanism by which LY293111 inhibits tumor growth is a matter of debate. In addition to its originally described inhibitory effects on the LTB₄ receptor, LY293111 has also been shown to be an agonist for the peroxisome proliferator-activated receptor γ (PPAR γ) and also a weak

5-LOX inhibitor. All three functions have been linked to the inhibition of cancer cell growth. It is possible that the anticancer effects of LY293111 involve all of these and perhaps even other unrecognized pathways, but this may make the drug even more useful in the clinic. LY293111 will, of course, exhibit some anti-inflammatory properties, but this is also likely to be valuable in the clinic.

The current study also demonstrates the importance of an adequate tumor model for testing new treatment options. It has been shown by Hoffman [31] that the orthotopic metastatic mouse model is a clinically relevant and appropriate tumor model for the evaluation of new anticancer drugs and, therefore, provides a bridge to clinical trials. We modified the model of SOI by injecting tumor cells into the duodenal part of the pancreas. With this modification, cancer development mimics the clinical course of pancreatic cancer in humans, including duodenal and bile duct obstruction. Moreover, the

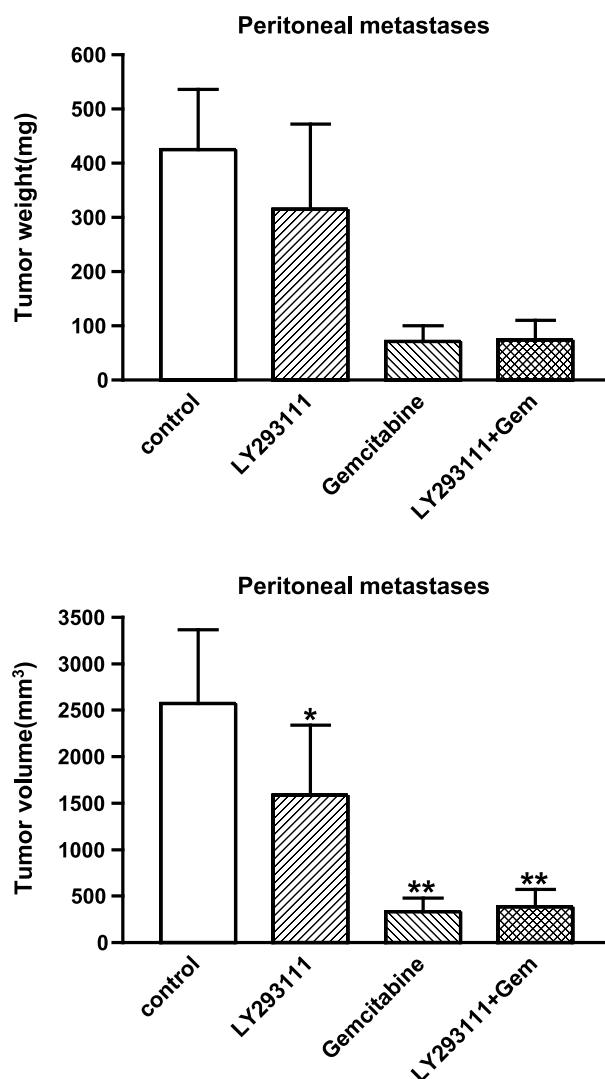


Figure 4. Peritoneal tumor weights and volumes (mean \pm SEM) 4 weeks after SOI of S2-013 GFP human pancreatic cancer cells. Groups include control; LY293111 (LY); (250 mg/kg per day); gemcitabine (Gem) (60 mg/kg per dose); and combined LY293111 and gemcitabine (LY + Gem) therapy. All P values are shown in Table 2.

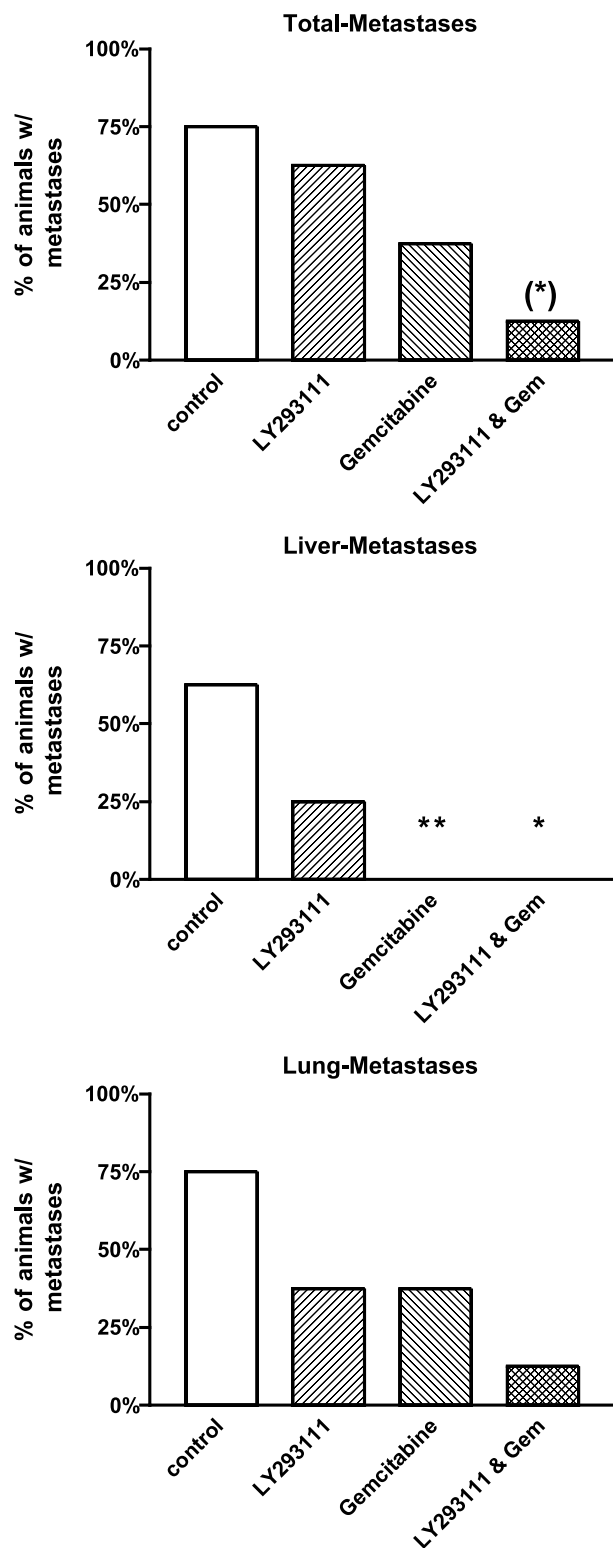


Figure 5. Occurrence of total organ, liver, and lung metastases 4 weeks after SOI of S2-013 GFP human pancreatic cancer cells, expressed as percentage of animals in each group. Groups include control; LY293111 (LY); (250 mg/kg per day); gemcitabine (Gem) (60 mg/kg per day); and combined LY293111 and gemcitabine (LY + Gem) therapy. All P values are shown in Table 2.

human pancreatic cancer cell line, S2-013, was chosen because of its aggressiveness and spontaneous development of liver, lung, and lymph node metastases. However, the

greatest advantage was provided by the stable expression of GFP and the application of the reversible skin flap, enabling us to study the course of tumor progression and development of metastases dynamically over time [29,25]. A scoring system was introduced in an attempt to improve on previous approaches with orthotopic models, which has been used to describe the presence or absence of metastases. The scoring system was prospectively developed by the investigators, and scoring was undertaken in a blinded fashion to prevent investigator bias. It should be noted that this scoring system has not been validated with regard to animal survival. Furthermore, we have no information on how it may parallel the TNM score in humans or future clinical experiences with this drug. Establishing the human TNM score was a long-term and slowly evolving process, involving multiple centers in several countries. If others adopt our scoring system or something similar, then this will perhaps provide the opportunity to develop and improve this scoring system.

In conclusion, LY293111 improves the efficacy of gemcitabine in an orthotopic model of human pancreatic adenocarcinoma.

References

- [1] Greenlee RT, Hill-Harmon MB, Murray T, and Thun M (2001). Cancer statistics, 2001. *CA Cancer J Clin* **51**, 15–36.
- [2] Lin Y, Tamakoshi A, Wakai K, Kawamura T, Aoki R, Kojima M, and Ohno Y (1998). Descriptive epidemiology of pancreatic cancer in Japan. *J Epidemiol* **8**, 52–59.
- [3] Oomi K and Amano M (1998). The epidemiology of pancreatic diseases in Japan. *Pancreas* **16**, 233–237.
- [4] Howard TJ (1996). Pancreatic adenocarcinoma. *Curr Probl Cancer* **20**, 281–328.
- [5] Yeo CJ and Cameron JL (1999). Improving results of pancreaticoduodenectomy for pancreatic cancer. *World J Surg* **23**, 907–912.
- [6] Ahrendt SA, and Pitt HA (2002). Surgical management of pancreatic cancer. *Oncology (Huntington)* **16**, 725–734.
- [7] Heinemann V (2001). Gemcitabine: progress in the treatment of pancreatic cancer. *Oncology* **60**, 8–18.
- [8] Abbruzzese JL (2002). New applications of gemcitabine and future directions in the management of pancreatic cancer. *Cancer* **95**, 941–945.
- [9] Tong WG, Ding XZ, Hennig R, Witt RC, Standop J, Pour PM, and Adrian TE (2002). Leukotriene B4 receptor antagonist LY293111 inhibits proliferation and induces apoptosis in human pancreatic cancer cells. *Clin Cancer Res* **8**, 3232–3242.
- [10] Hennig R, Ding XZ, Tong WG, Schneider MB, Standop J, Friess H, Buchler MW, Pour PM, and Adrian TE (2002). 5-Lipoxygenase and leukotriene B(4) receptor are expressed in human pancreatic cancers but not in pancreatic ducts in normal tissue. *Am J Pathol* **161**, 421–428.
- [11] Tong W-G, Ding X-Z, and Adrian TE (2001). The leukotriene B4 receptor antagonist, LY293111 induces apoptosis through the mitochondrial pathway in human pancreatic cancer cells. *Pancreas* **23**, 465.
- [12] Tong W-G, Ding X-Z, and Adrian TE (2002). Involvement of the MAPK and PI3 kinase pathways in leukotriene B4 stimulated human pancreatic cancer cell proliferation. *Pancreas* **25**, 453.
- [13] Funk CD (2001). Prostaglandins and leukotrienes: advances in eicosanoid biology. *Science* **294**, 1871–1875.
- [14] Sampson AP (2000). The role of eosinophils and neutrophils in inflammation. *Clin Exp Allergy* **30** (Suppl 1), 22–27.
- [15] Ding XZ, Tong WG, and Adrian TE (2001). Cyclooxygenases and lipoxygenases as potential targets for treatment of pancreatic cancer. *Pancreatology* **1**, 291–299.
- [16] Ding XZ and Adrian TE (2001). Role of lipoxygenase pathways in the regulation of pancreatic cancer cell proliferation and survival. *Inflammopharmacology* **00**, 1–8.
- [17] Sawyer JS, Bach NJ, Baker SR, Baldwin RF, Borrromeo PS, Cockerham SL, Fleisch JH, Floreancig P, Froelich LL, and Jackson WT (1995). Synthetic and structure/activity studies on acid-substituted

- 2-arylphenols: discovery of 2-[2-propyl-3-[3-[2-ethyl-4-(4-fluorophenyl)-5-hydroxyphenoxy]-propoxy]phenoxy]benzoic acid, a high-affinity leukotriene B4 receptor antagonist. *J Med Chem* **38**, 4411–4432.
- [18] Jackson WT, Froelich LL, Boyd RJ, Schrementi JP, Saussy DL, Jr, Schultz RM, Sawyer JS, Sofia MJ, Herron DK, Goodson T, Jr, et al. (1999). Pharmacologic actions of the second-generation leukotriene B4 receptor antagonist LY293111: *in vitro* studies. *J Pharmacol Exp Ther* **288**, 286–294.
- [19] Mommers JM, Van Rossum MM, Kooijmans-Otero ME, Parker GL, and van de Kerkhof PC (2000). VML 295 (LY-293111), a novel LTB4 antagonist, is not effective in the prevention of relapse in psoriasis. *Br J Dermatol* **142**, 259–266.
- [20] van Pelt JP, de Jong EM, van Erp PE, Mitchell MI, Marder P, Spaethe SM, van Hooijdonk CA, Kuijpers AL, and van de Kerkhof PC (1997). The regulation of CD11b integrin levels on human blood leukocytes and leukotriene B4-stimulated skin by a specific leukotriene B4 receptor antagonist (LY293111). *Biochem Pharmacol* **53**, 1005–1012.
- [21] van Pelt JP, de Jong EM, Seijger MM, van Hooijdonk CA, De Bakker ES, Van Vlijmen IM, Parker GL, van Erp PE, and van de Kerkhof PC (1998). Investigation on a novel and specific leukotriene B4 receptor antagonist in the treatment of stable plaque psoriasis. *Br J Dermatol* **139**, 396–402.
- [22] Ding XZ, Fehsenfeld DM, Murphy LO, Permert J, and Adrian TE (2000). Physiological concentrations of insulin augment pancreatic cancer cell proliferation and glucose utilization by activating MAP kinase, PI3 kinase and enhancing GLUT-1 expression. *Pancreas* **21**, 310–320.
- [23] Schmied BM, Ulrich AB, Matsuzaki H, El Metwally TH, Ding X, Fernandes ME, Adrian TE, Chaney WG, Batra SK, Pour PM (2000). Biologic instability of pancreatic cancer xenografts in the nude mouse. *Carcinogenesis* **21**, 1121–1127.
- [24] Bouvet M, Wang J, Nardin SR, Nassirpour R, Yang M, Baranov E, Jiang P, Moossa AR, and Hoffman RM (2002). Real-time optical imaging of primary tumor growth and multiple metastatic events in a pancreatic cancer orthotopic model. *Cancer Res* **62**, 1534–1540.
- [25] Hoffman R (2002). Green fluorescent protein imaging of tumour growth, metastasis, and angiogenesis in mouse models. *Lancet Oncol* **3**, 546–556.
- [26] Yamanari H, Sukanuma T, Iwamura T, Kitamura N, Taniguchi S, and Setoguchi T (1994). Extracellular matrix components regulating glandular differentiation and the formation of basal lamina of a human pancreatic cancer cell line *in vitro*. *Exp Cell Res* **211**, 175–182.
- [27] Iwamura T, Katsuki T, and Ide K (1987). Establishment and characterization of a human pancreatic cancer cell line (SUIT-2) producing carcinoembryonic antigen and carbohydrate antigen 19-9. *Jpn J Cancer Res* **78**, 54–62.
- [28] Iwamura T, Caffrey TC, Kitamura N, Yamanari H, Setoguchi T, and Hollingsworth MA (1997). P-selectin expression in a metastatic pancreatic tumor cell line (SUIT-2). *Cancer Res* **57**, 1206–1212.
- [29] Yang M, Baranov E, Wang JW, Jiang P, Wang X, Sun FX, Bouvet M, Moossa AR, Penman S, and Hoffman RM (2002). Direct external imaging of nascent cancer, tumor progression, angiogenesis, and metastasis on internal organs in the fluorescent orthotopic model. *Proc Natl Acad Sci USA* **99**, 3824–3829.
- [30] Sun FX, Tohgo A, Bouvet M, Yagi S, Nassirpour R, Moossa AR, and Hoffman RM (2003). Efficacy of camptothecin analog DX-8951f (exatecan mesylate) on human pancreatic cancer in an orthotopic metastatic model. *Cancer Res* **63**, 80–85.
- [31] Hoffman RM (1999). Orthotopic metastatic mouse models for anti-cancer drug discovery and evaluation: a bridge to the clinic. *Invest New Drugs* **17**, 343–359.